Am J Transl Res 2021;13(10):11065-11080
www.ajtr.org /ISSN:1943-8141/AJTR0133814

Original Article

LncRNA HAGLR absorbing miR-214-3p promotes BMP2 expression and improves tibial fractures

Jinlong Chen, Yishan Yang

Department of Orthopedics, Zhangzhou Affiliated Hospital of Fujian Medical University, Zhangzhou 363000, Fujian Province, China

Received April 1, 2021; Accepted August 29, 2021; Epub October 15, 2021; Published October 30, 2021

Abstract: Objective: To determine whether long-chain non-coding RNA (lncRNA) HAGLR can regulate BMP2 by absorbing microRNA-214-3p (miR-214-3p), and to explore its role and mechanism in tibial fracture (TF) healing. Methods: The HAGLR, miR-214-3p, and BMP2 expression levels in TF and in adjacent normal tissues were measured using quantitative real-time polymerase chain reaction (qRT-PCR). MC3T3-E1 osteoblasts were used to construct the *in vitro* model. HAGLR was localized subcellularly through RNA-fluorescence in situ hybridization (FISH). A dual-luciferase report experiment confirmed that miR-214-3p has a targeted relationship with HAGLR and BMP2. It was then divided into a HAGLR over-expression group, an miR-214-3p mimic group, a HAGLR+miR-214-3p mimic group, an sh-HAGLR group, a BMP over-expression group, an sh-HAGLR+over-expression BMP2 group, and a negative control group. The proliferation and apoptosis of the MC3T3-E1 osteoblasts were examined using MTT assays and flow cytometry. A TF model was established in male C57BL/6J mice. The serum alkaline phosphatase (ALP) and osteoprotegerin (OPG) levels in the sham group, the TF group, and the TF group that were injected with HAGLR were compared using ELISA. Hematoxylin-eosin (HE) staining was used to confirm the fracture healing in the mouse model. Results: Compared with the adjacent normal tissues in the TF patients, the HAGLR and BMP2 expressions decreased but the miR-214-3p expressions increased in the TF tissues ($P<0.05$). HAGLR, an endogenous sponge, absorbed the miR-214-3p, and the BMP2 expression was directly regulated by miR-214-3p. HAGLR increased the proliferative activity of the osteoblasts and decreased the apoptosis rate. The over-expression of miR-214-3p partly reversed the effect of HAGLR on the cells, decreased the proliferative activity, and increased the apoptosis rate (all $P<0.05$). The sh-HAGLR decreased the proliferative activity and increased the apoptosis rate. But after the over-expression of BMP2, the proliferative activity of the cells was higher, and the apoptosis rate was lower than it was in the sh-HAGLR group (all $P<0.05$). The over-expression of HAGLR can up-regulate the ALP and OPG levels in mouse models ($P<0.05$). Conclusion: lncRNA HAGLR can regulate BMP2 to play a protective role in TF by absorbing miR-214-3p, and it is related to promoting the osteoblast proliferation, inhibiting apoptosis, and up-regulating the serum ALP and OPG levels to accelerate bone healing.

Keywords: Tibial fractures, lncRNA HAGLR, osteoblasts, apoptosis, proliferation

Introduction

Tibial fractures (TF) are considered to be the most common form of traumatic fracture, and they will lead to a permanent decrease in bone density. Postoperative TF patients often also suffer from limb deformities, joint dysfunction etc. [1, 2]. Bone formation, remodeling and healing are highly regulated and extremely complex processes, which requires the coordination of different types of cells [3]. Osteoblast-mediated delayed bone formation will lead to delayed fracture healing [4]. Although surgery is the first choice for treating tibial fractures, it's difficult to treat intra-articular fractures surgically. So, it is still a great challenge for trauma surgeons to ensure positive treatment results [5].

It has been found that long chain non-coding RNAs (LncRNAs) play an important role in fracture healing [6]. Previous studies have shown that the expression of LncRNA HAGLR is down-regulated in patients with femoral neck fractures (FNF). HAGLR can promote the survival rate and migration of MC3T3-E1 cells, inhibit

apoptosis, and up-regulate the activity of osteoblasts [7], but its role in TF is unclear, so that is the focus of this research.

microRNA (miRNA) has the ability to regulate the expressions of many genes, and it is related to many physiological functions and disease processes [8]. Research has shown that miRNAs can play a key role in the process of osteoarthritis after TF by regulating the target genes, and their functions almost always involve proliferation, differentiation, aging, and the apoptosis of cell processes [9]. Research has also suggested that the amounts of callus and osteocalcin in mice decreases after the injection of miR-214-3p, which can delay the healing of TF by inhibiting the Wnt/β-catenin signaling pathway [10].

BMP2 is a crucial member of the transforming growth factor-β family [11]. Research shows that BMP2 expression is significantly decreased in patients with delayed bone healing [12]. In addition, BMP2 is involved in cartilage formation and stimulates bone marrow mesenchymal stem cells to differentiate into osteoblasts to accelerate fracture healing [13]. Therefore, the BMP2 expression will affect fracture healing and callus formation.

The purpose and innovation of this study is to show the role of lncRNA HAGLR in TF and disclose its possible mechanism for the first time, in order to provide a new and targeted molecular therapeutical treatment strategy.

Materials and methods

Ethical statement

This research was approved by the ethics committee of our hospital. With the informed consent of each patient, their clinical data records were renumbered to keep them secret. The animal experiment scheme was examined and approved by the animal ethics committee of our hospital, and the experimental operation was carried out strictly in accordance with the guidelines for the nursing and use of experimental animals formulated by the National Institutes of Health.

Collection of the TF tissue samples

From January 2019 to August 2020, 42 patients with complex tibial plateau fractures diagnosed through CT in our hospital were recruited as the research cohort. There were 28 male and 14 female patients, and they ranged in age from 34 to 75 years old, with an average age of 52.1 years old. There were 17 cases of open fractures and 25 of closed fractures. The fractured bones and the adjacent normal tissues were stored in liquid nitrogen. Inclusion criteria: (1) all the patients were diagnosed with tibial plateau fractures through CT examinations, (2) patients with unhealed fractures within the previous 4 months and whose X-ray images showed that the fracture line was blurred and there was continuous callus, and (3) patients with relatively complete clinical data [14]. Exclusion criteria (1) patients with a history of tibial plateau fractures or surgical operations, (2) patients with dysfunction of the vital organs such as the heart, liver, and kidneys, (3) patients comorbid with malignancies, and (4) patients who had participated in other research projects.

Cell culture and transfection

MC3T3-E1 osteoblasts were purchased from the American Type Culture Collection (ATCC), and the cells were frozen in an RPMI 1640 (12633012, Thermo Fisher Scientific, Inc. USA) medium containing 40% fetal bovine serum (FBS) (16000-077, Gibco, USA) and 5% dimethyl sulfoxide (methyl sulfoxide, DMSO) (D2650, Sigma-Aldrich, USA) according to the instructions. They were shaken and thawed in a water bath at 37°C, and then centrifuged at 1000 rpm for 3 min. The supernatant was discarded, and 1 mL of culture medium was mixed in and blew well. Next, all the cell suspensions were transferred to a flask containing 5 mL culture medium and cultured overnight. The cells were sub-cultured after reaching 80%-90% confluency. The cells in the logarithmic growth phase were digested with 0.25% pancreatin (PB180224, Procell, China), then inoculated into a 6-well plate (A1098202, Thermo Fisher Scientific, Inc. USA), and cultivated in a 5% CO_2 incubator at 37°C all night long. The lentivirus against lncRNA HAGLR (sh-lncRNA HAGLR) and the negative control (sh-HAGLR-NC) were designed and constructed by Shanghai Gene Co., Ltd. A lentivirus packaging system plasmid was prepared, then MC3T3-E1 cells were co-infected and the virus was packaged, and the virus-containing supernatant was collected. In a 40 mL ultracentrifuge tube,

Table 1. Vector sequence for the transfection

Name		Sequences (5'-3')
sh-HAGLR-NC	Sense strand	5'-ACTGCCCTGATGCTAGCTAGCACCGGT-3'
	Antisense strand	5'-GCUCGATCCTGCTAGATCUUCGCUAC-3'
sh-HAGLR	Sense strand	5'-GGUCGAUUGAUUGCAUCUATT-3'
	Antisense strand	5'-UAGCUC UAACCAGAGACAUTT-3'
pcDNA3.1-BMP2	Forward	5'-TAGAATCTTCTTTTCGACGAAGATGTATGA-3'
	Reverse	5'-CTTGAACGGATTGTGATATACCCCTTACAG-3'
pcDNA3.1-HAGLR	Forward	5'-TATTCTTTGAATCTCGACGAAGATGTATGA-3'
	Reverse	5'-CTTGAACGGATTGTGATATACCCCTTACGA-3'
mimic-NC	Forward	5'-UCUCAGCGUCGUCAUUCGATT-3'
	Reverse	5'-ACAACGAGGAAUUUCGGGCTT-3'
miR-214-3p mimic	Forward	5'-UAGCCAGAGGUGCCGUGAAC-3'
	Reverse	5'-CCGACUUACUGUUCGACCUU-3'

the cells were centrifuged at 80,000 rpm, at 4°C for 2 h, resuspended in pre-cooled PBS, and dissolved at 4°C overnight. When the fusion degree of MC3T3-E1 cells reached 60%-70%, sh-HAGLR and sh-HAGLR-NC were dropped on the cell surface respectively. After 8 h, they were changed into a normal DMEM medium containing 10% FBS. The full-length sequences of BMP2 and HAGLR were cloned into a pcDNA3.1 vector, and high expression vectors of BMP2 (pcDNA3.1-BMP2) and HAGLR (pcDNA3.1-HAGLR) were constructed. The miR-214-3p mimic and its matched negative control (mimic-NC) were designed and synthesized by Shanghai GenePharma. The cells were transfected using a LipofectamineTM 3000 (L3000015, Invitrogen, USA) transfection reagent based on the instructions. After that, the cells were incubated in an incubator at 37°C and 5% CO_2 for the subsequent experiments. The sequences of the transfected vectors are shown in **Table 1**.

Fluorescence in situ hybridization test

In the MC3T3-E1 osteoblasts, whether lncRNA HAGLR was located in the nuclei or cytoplasms was determined using fluorescence in situ hybridization (FISH): the MC3T3-E1 cells were sliced and washed 2-3 times in PBS, for five minutes each time. At 4°C, they were fixed with 4% paraformaldehyde for 5-10 min and rinsed with PBS. Then, 0.5% TritonX-100 permeable liquid (P0096, Beyotime, China) was added, and the cells were incubated for 20 min and rinsed for 10 min in PBS. Afterwards, absolute alcohol was added and dried, and a hybridization solution (Xishitan Town) was supplemented. The probe was put on a PCR instrument and denatured, and then it was added to the culture hole for immersion climbing. Subsequently, the cells were incubated at 37°C overnight, rinsed and then mixed with 3% BSA dropwise and blocked. A digoxin fluorescent secondary antibody was added. Subsequently, they were incubated for 1 h and dyed for 10 min with DAPI (4'-6-diamidino-2-phenylindole) staining solution (C1006, Beyotime, China). Afterwards, they were cleaned again with PBS solution for 15-20 min, then we washed off the excess PBS with clear water, and then we dried the cells at room temperature. The cells were protected from light and sealed. Finally, they were observed under a fluorescence microscope and captured and photographed (CKX53, Olympus, Japan).

Dual-luciferase report analysis

The targeted relationship between miR-214-3p and HAGLR or BMP2 was predicted through the LncSNP online prediction target website (http://210.46.80.146/lincsnp/search.php). The luciferase activity was measured according to the instructions of dual-luciferase reporter assay kit (RG027, Beyotime, China). The sequence containing the miR-214-3p binding site on HAGLR or BMP2 3' (the untranslated region) UTR was amplified using PCR and cloned into a luciferase vector and recorded as HAGLR-WT or BMP2-WT (Wild type). At the same time, PCR amplified the mutant sequences and were cloned into mutant plasmids, which were named HAGLR-MUT or BMP2-MUT (the mutant type). In view of the instructions of

Table 2. The qRT-PCR sequences

Name		Sequences (5'-3')
lncRNA HAGLR	Forward	GAATGGATATDCTGGGTTTC
	Reverse	TACATGAAATCGATCTTGCCG
miR-214-3p	Forward	CGTTAACAGCTGTACCATC
	Reverse	AGTGATGGTGTAGGTGTAGG
BMP2	Forward	TCACTAGTAGCAAACCCACGT
	Reverse	TTCTTCCCTTGGTATCTATCTCG
GAPDH	Forward	CTCACTGCTACATCCAGTACAC
	Reverse	CCTGCCTACCATGTTT ACC G
U6	Forward	ACGCAUCAUAGUUAUGCACCAAAUG
	Reverse	GUAUACUUGGCUCGCUCCG AUAU

Lipofectamine™ 3000 (L3000015, Invitrogen, USA), the mimic-NC or miR-214-3pmimic and luciferase plasmids were transfected into MC3T3-E1 cells in groups. Forty-eight hours after the transfection, the old culture medium was discarded. The cells were washed with PBS 2-3 times, and 100 μL lysis buffer was added to each well and then shaken for 15 min in a table concentrator. The cell lysate was collected and centrifuged at 10000 rpm for 3 min. Then, 50 μL firefly luciferase reaction solution and 50 μL sea cucumber luciferase reaction solution were added, and they were mixed quickly and evenly, and then we put them into a luminescent plate for quantification and reading. Each experiment was repeated 3 times. The luciferase activity of the fireflies in the transfected cells was tested using a microplate reader (TekELX800, BioTEK, USA). With the sea kidney luciferase activity as the internal control, the relative luciferase activity was the ratio of the firefly luciferase activity to the sea kidney luciferase activity.

Quantitative real-time polymerase chain reaction (RT-PCR)

The cells were incubated for 48 h after the transfection and were then collected, and the total RNA was extracted using Trizol reagent (15596018, Invitrogen, USA) based on the kit instructions. The cDNA was synthesized from the tissues and cell samples using a reverse transcription kit (RR037A, TaKaRa, Japan). The reaction system was described with reference to the reverse transcription kit, and the conditions were as follows: incubation at 37°C for 0.5 h, 85°C for 10 s and standing at 4°C for 10 min. After the reaction was terminated, a TaqMan Universal Master Mix II (4440043, Thermo Fisher, USA) was used to carry out the real-time quantitative PCR. The reaction system was as follows (total volume 20 μL): 2×Taqman Universal Master Mix II 10 μL, Rnase Free ddH_2O 8 μL, cDNA template 1 uL, 20×Taqman Assay 1 μL. The real-time quantitative PCR reaction conditions were as follows: 95°C, 10 min, 95°C, 30 s, 95°C, 5 s, 60°C, 34 seconds. A total of 45 cycles were amplified. GAPDH was regarded as the internal reference of LncRNA HAGLR and BMP2, and U6 was used as an internal reference of Mir-214-3p. The relative expression levels were calculated using $2^{-\Delta\Delta CT}$. The tissue test procedure was the same. The gene sequences were retrieved from the Shengxin database and the primers were designed. The primer sequences are shown in **Table 2**.

Western blot (WB)

Forty-eight hours after the transfection, the cells in each group were collected, lysed by adding 1% Triton-100 on ice, and centrifuged at 12000 RPM at 4°C for 10 min, and then the supernatant was collected. The steps were strictly carried out according to the (R0010, Solarbio, China) instructions of the protein extraction kit. After the BCA was quantified, 30 μg of protein was extracted and separated using SD-SPAGE gel electrophoresis. The voltages in the concentrated gel and separated gel were 80 V and 120 V respectively. After the electrophoresis, the separation gel was soaked in a membrane transfer solution, and transferred to a PVDF membrane. The membrane was placed in TBST sealing solution and sealed for 2 h. It was taken out again and washed 2-3 times in TBST, 5 min each time. Primary antibody BMP2 was added (1:1000; ab214821, Abcam, UK), incubated at 4°C for more than 15 h, and washed with TBST solution 2-3 times the next day, five minutes each time. Horseradish peroxidase (HRP) labelled second antibody IgG (1:2000; abab6721, Abcam, UK) was added, then it was reacted at room temperature in a table concentrator for 2 h, and then the membrane was cleaned with TBST. The samples were measured using enhanced chemiluminescence (ECL), developed in an ECL color-substrate solution (WBKIS0100, Millipore, USA), and then fixed with a fixing solution. Image J software was used for the gray analysis, and

protein level = target band gray value/internal reference protein (GAPDH) band gray value.

MTT test

The cell proliferation activity was examined using MTT assays. The transfected MC3T3-E1 cells in the logarithmic growth phase were collected, then they were digested with 0.25% trypsin, and then they were added to a 96-well plate with the adjusted concentration. After the cell attachment, 10 μL MTT solution (PB180519, Procell, China) was added at 0, 24, 48, and 72 h, respectively, and the supernatant was discarded after incubation for 4 h. Then, 150 μL DMSO solution (D2650, Sigma, USA) was added, and the cells were shaken at room temperature for 5 min under dark conditions. The absorbance (OD) at a wavelength of 450 nm was measured using a microplate reader (TekELX800, Bio-TEK, USA).

Flow cytometry analysis

The apoptosis of the cells was tested using the Annexin V/PI dual staining kit (BB-4101, BestBio, China). First, the cells were collected and digested with 0.25% trypsin without EDTA to prepare a single cell suspension. Next, they were centrifuged for 5 min at 800 RPM. Finally, the supernatant was discarded. After the cells were cleaned with PBS, precooled 70% ethanol was added, fixed at 4°C and centrifuged again for 5 min. The lower layer cells were washed with PBS solution and then sieved and resuspended. FITC labeled Annexin V was added at room temperature, mixed gently, and reacted for 15 min. Afterwards, PI dye liquor was added, incubated for 5 min away from light, and then measured using flow cytometry (DxFLEX, Beckman, USA).

TF model establishment

Sixty clean healthy male C57BL/6 mice (12 weeks old, weighing 25-30 g) were randomly selected from the Hunan Experimental Animal Research Center (License for use of laboratory animals: SYXK (Xiang) 2012-0004). The rats were randomized into 3 groups: a sham group (n=5, the sham operation group, only anesthesia without an operation), a TF group (n=5, a TF operation after anesthesia), and a pc-HAGLR group (n=5, after modeling, 5 μL pc-HAGLR was injected directly around the fracture site). Mouse TF models were established according to previously published studies [15]. The mice were exposed to 2% isoflurane (26675-46-7, Macklin, China) in a transparent anesthetic box. The mice in all the groups except the sham group were anesthetized, depilated, disinfected, and skinned. Then the left tibia of the mice was exposed, and holes were drilled in the middle of the tibia, and 0.1 mm bone nails were inserted along the direction of bone marrow cavity for fixation. After the transverse stage, the incision was closed and injected accordingly. The sham group was also administered isoflurane anesthesia in the lateral tibia incision surgery, and the incision was sutured after peeling off periosteum. Afterwards, the mice in each group were given compound lidocaine gel ointment to relieve their inflammation and pain.

Enzyme-linked immunosorbent assay (ELISA)

Forty-eight hours after the operations, blood samples were collected from the submandibular vein in the fasting mice in each group (5 in each group). Before the blood collection, mice were anesthetized with fentanyl 20 μg/kg+ droperidol 500 μg/kg to relieve the animals' pain, and 0.5 mL was collected from each mouse. The venous blood was transferred to the anticoagulant EP tube, and the supernatant was obtained after 3000 rpm centrifugation for 10 min. The levels of alkaline phosphatase (ALP) and osteoprotegerin (OPG) in the mouse serum were compared using ELISA. The specific operation steps were carried out strictly in accordance with the enzyme labeling instrument (TekELX800, Bio-TEK, USA), the supporting ALP detection kit (SP11042, Saipei Bio, China), and the OPG detection kit (SP10950, Saipei Bio, China) instructions.

HE staining

First, the mice were anesthetized with 2% pentobarbital sodium and then sacrificed by cervical dislocation (5 in each group). The tibia tissues of each group were obtained by soaking them in 75% ethanol (D885934, Macklin, China) for 5 min in an aseptic environment at room temperature.

The specific procedures: The skin was cut through a small orifice of 2-3 cm to the lateral thigh, and the abdominal skin was dissociated. Then, the skin was cut and fixed with tweezers. The Achilles tendon was cut off, and the tibial head was fixed with tweezers. The free tibia

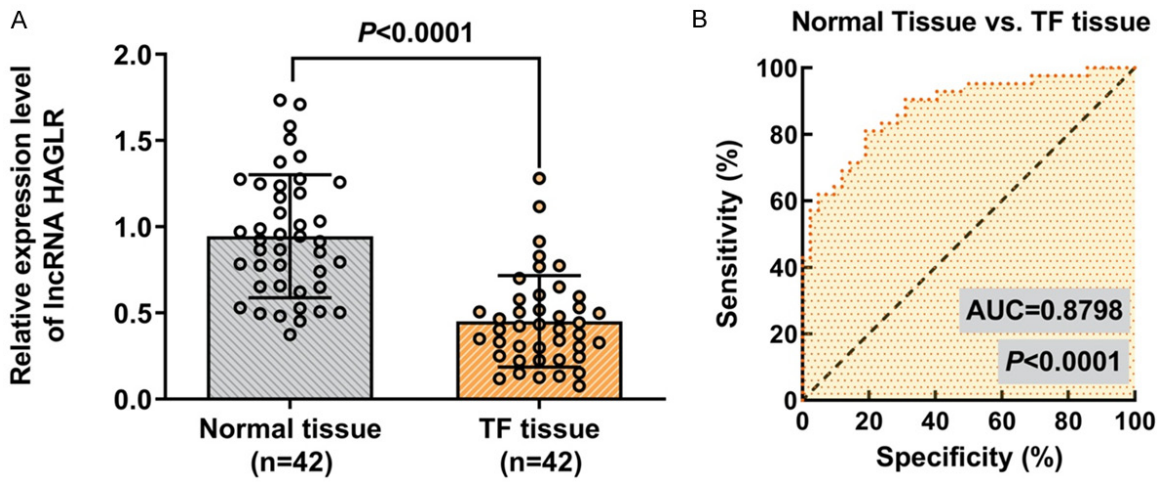

Figure 1. The relative expression of lncRNA HAGLR. A: The expression of HAGLR in the TF tissues (n=42) and adjacent normal tissues (n=42) is measured using qRT-PCR; B: A diagnostic value curve (AUC=0.8798, 95% CI: 0.8076-0.9520, *P*<0.0001).

was exposed to the callus. The tibia was amputated 1 cm away from the callus, and the callus was left. It was rinsed in a Petri dish containing 4-10°C and 10 mL PBS solution. After fixation with neutral formaldehyde, 15% Ethylenediaminetetraacetic acid (EDTA) (E809068, Macklin, China) was decalcified for 4 weeks, and then dehydrated and embedded in paraffin. A 3 um tissue section was cut continuously. The slices were baked overnight at 60°C and then made into tissue sections. Hematoxylin-eosin staining was used for the histological observation. After dehydration with gradient ethanol, the cells were stained with hematoxylin dye solution (G1080, Solarbio, China) for 5 min and rinsed with running water. Afterwards, the sections were immersed in PBS, rinsed 3 times in pure water until it was fully blue, then dyed with eosin solution (G1100, Solarbio, China) for 3 min, and then subjected to gradient dehydration again. Finally, they were placed in xylene (4463-44-9, Aladdin, China) for 5 min and sealed with neutral resin. Next, under a 400× microscope, five visual fields were randomized from each specimen and the osteoblasts in the visual field were observed. The number of osteoblasts per unit area (mm^2) was calculated and recorded.

Statistical analysis

In this research, the data were statistically analyzed using SPSS 22.0 software. All the measurement data with a normal distribution and uniform variance were expressed in the form of the mean ± standard deviation ($\bar{x}$±sd). The comparisons between two groups were carried out using independent samples t-tests, and ANOVA followed by Bonferroni post-hoc tests were used for the comparisons among multiple groups. The count data were expressed as a percentage and analyzed using Pearson Chi-square tests. If it did not conform to a normal distribution or homogeneity of variance, a rank sum test was performed, and the diagnostic value was analyzed using the Kaplan Meier method. *P*<0.05 indicated that a difference was statistically significant.

Results

lncRNA HAGLR expressions were decreased in the TF tissues

The expressions of HAGLR in the TF tissues were measured using the qRT-PCR method. Compared with the adjacent normal tissues (n=42), the HAGLR expressions in the TF tissues were lower (n=42) (**Figure 1A**, *P*<0.001). Meanwhile, our ROC curve analysis indicated that the area under the ROC curve of HAGLR in predicting TF was 0.8798 (**Figure 1B**) (AUC= 0.8798, 95% CI: 0.8076-0.9520, *P*<0.0001). To sum up, it can be concluded that HAGLR can be used as an effective molecular diagnostic index for TF.

HAGLR promoted the proliferation of the osteoblasts and inhibited their apoptosis

To observe the potential effect of HAGLR on the osteoblasts, MC3T3-E1 cells were trans-

fected with a HAGLR overexpression or knockdown vector. It showed that the expression of HAGLR was higher than it was in the negative control group (**Figure 2A**, $P<0.05$), and shRNA could effectively inhibit the expression of HAGLR ($P<0.05$). The MTT assay results showed that the proliferative activity of the MC3T3-E1 cells was enhanced after the overexpression of HAGLR (**Figure 2B**, $P<0.05$). The flow cytometry results revealed that the number of apoptotic cells decreased sharply after we increased the HAGLR expression in the MC3T3-E1 cells (**Figure 2C**, $P<0.05$). In addition, the HAGLR knockdown was able to stimulate apoptosis and inhibit the proliferation of the MC3T3-E1 cells (**Figure 2B**, **2C**, $P<0.05$).

HAGLR was mainly located in the cytoplasms and was able to regulate its expression in the osteoblasts by absorbing miR-214-3p

miR-214-3p with a targeted binding site to lncRNA HAGLR was predicted using an online bioinformatics prediction website analysis (**Figure 3A**). In situ hybridization showed DAPI labeled nuclei and fluorescence in situ labeled HAGLR molecules. The combined images signified that HAGLR molecules were mainly located in the cytoplasm (**Figure 3B**). According to the predicted target of the website, A dual-luciferase reporter genetic analysis revealed that the over-expression of miR-214-3p inhibited the luciferase activity in the wild-type HAGLR vector and verified the binding of HAGLR to miRNA-214-3p (**Figure 3C**, $P<0.05$). Compared with the adjacent normal tissues (n=42), miR-214-3p was highly expressed in the TF tissues (n=42) (**Figure 3D**, $P<0.001$). A Spearman correlation analysis revealed that it was negatively correlated with the expression of HAGLR in the TF tissues (n=42) (**Figure 3E**, r=-0.4002, $P<0.001$).

Also, the miR-214-3p expression in the MC3T3-E1 cells was up-regulated after the transfection with sh-HAGLR (**Figure 3F**, $P<0.05$), and the expression was down-regulated after the over-expression of HAGLR ($P<0.05$). It is suggested that miR-214-3p may be the target of HAGLR in the osteoblasts and may participate in the healing process of TF regulated by HAGLR.

miR-214-3p inhibited osteoblast proliferation and induced apoptosis

To further verify our hypothesis, the expression of miR-214-3p in each group of cells was measured using qRT-PCR. The miR-214-3p mimic dramatically up-regulated the expression of miR-214-3p, which was partially reversed by the transfection of pcDNA3.1-HAGLR (**Figure 4A**, all $P<0.05$). miR-214-3p inhibited the proliferation of the MC3T3-E1 cells (**Figure 4B**, $P<0.05$) and increased the rate of the apoptosis (**Figure 4C**, $P<0.05$). Thus, miR-214-3p can inhibit TF, but this effect can be partially reversed using pcDNA3.1-HAGLR (**Figure 4A-C**, $P<0.05$).

BMP2 was proved to be a target of miR-214-3p, which was expressed at low levels in the TF tissues

To further explore the mechanism of lncRNA HAGLR in promoting TF bone healing, we continued to search for possible regulatory targets of HAGLR/miR-214-3p, and screened and identified the target gene of miR-214-3p using the StarBase targeted relationship online prediction website. In this experiment, BMP2 was selected as a research object (**Figure 5A**). The interaction between BMP2 and the top 15 risk genes related to increased fracture probability found on the website of DisGeNET (http://disgenet.org/search) was analyzed. The results showed that BMP2 was relevant to the risk genes of increased fracture probability, which further confirmed the rationality of choosing to study BMP2 (**Figure 5B**). The qRT-PCR results revealed that the BMP2 expression in the TF tissues was down-regulated compared with the adjacent healthy tissues (**Figure 5D**, $P<0.001$). The Dual-luciferase report experiment further verified the targeted relationship between them (**Figure 5C**). miR-214-3p down-regulated the BMP2 expression, while lncRNA HAGLR partially reversed this trend (**Figure 5E**, **5F**, all $P<0.05$). At the same time, this shows that HAGLR can absorb miR-214-3p and regulate BMP2.

BMP2 over-expression reversed the inhibition of sh-HAGLR on osteoblast growth

The MTT and flow cytometry results (**Figure 6**) indicated that over-expressing BMP2 could significantly reverse the inhibitory effect of sh-HAGLR on osteoblast proliferation ($P<0.05$)

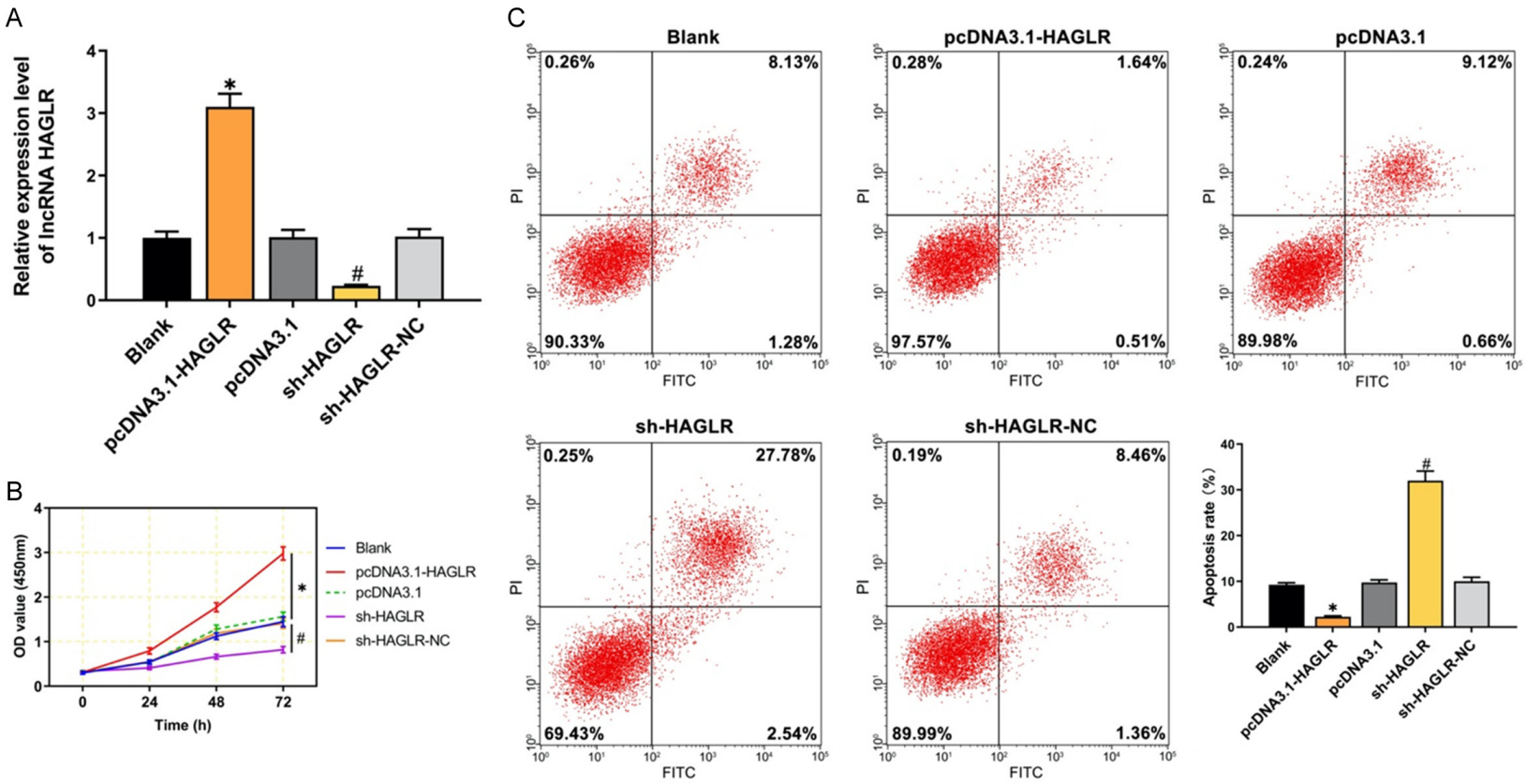

Figure 2. The effect of HAGLR on the proliferation and apoptosis of the osteoblasts. A: The expression of HAGLR after the transfection; B: The proliferation of the MC3T3-E1 cells was measured using MTT assays; C: The apoptosis of the MC3T3-E1 cells was measured using flow cytometry. Compared with the pcDNA3.1 group, $^{*}P<0.05$; compared with the sh-HAGLR-NC group, $^{\#}P<0.05$; n=3.

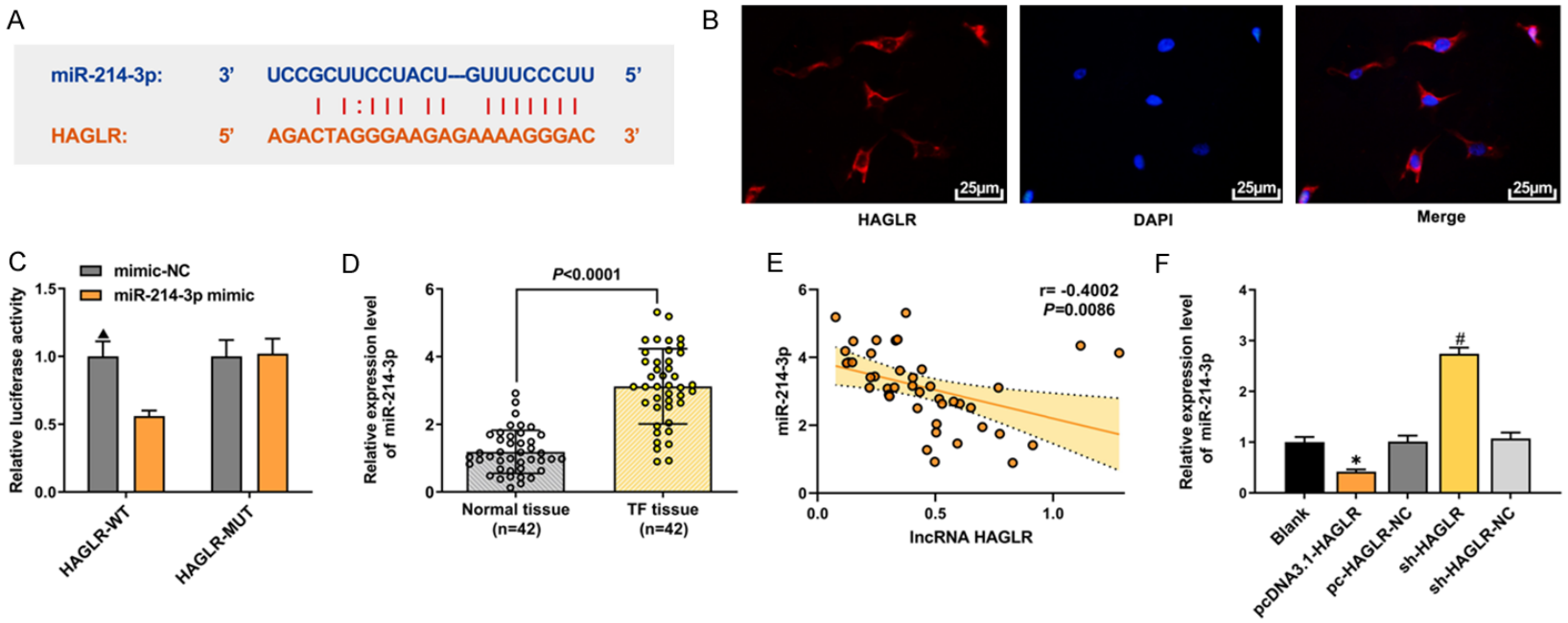

Figure 3. HAGLR absorbed miR-214-3p to regulate its expression in osteoblasts. A: The prediction from the LncSNP website (http://210.46.80.146/lincsnp/search.php); B: Fluorescence in situ hybridization (400×); C: Dual-luciferase reporter assay; D: qRT-PCR is used to determine the expression of miR-214-3p in the adjacent healthy tissues (n=42) and the TF tissues (n=42); E: Correlation analysis; F: The expression of miR-214-3p in the cells after the HAGLR intervention is measured using qRT-PCR; compared with the mimic-NC group, ▲P<0.05; compared with the pcDNA3.1 group, *P<0.05; compared with the sh-HAGLR-NC group, #P<0.05; n=3.

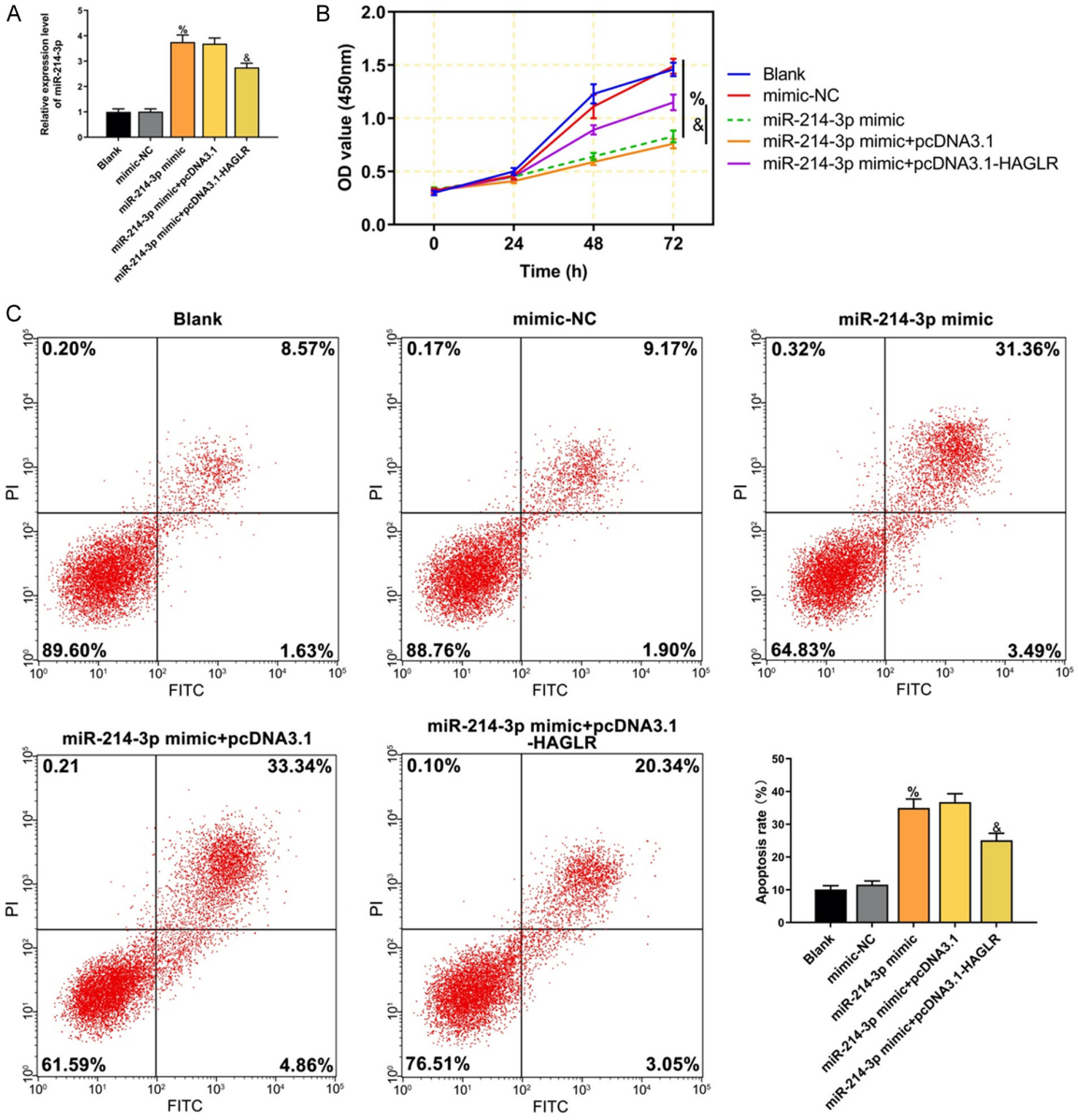

Figure 4. The role of HAGLR in the osteoblastic growth. A: The expression of miR-214-3p in the cells was measured using qRT-PCR; B: MTT assays are used to measure the cell proliferation; C: The apoptosis was measured using flow cytometry. Compared with the mimic-NC group, $^{\%}P<0.05$; compared with the miR-214-3p mimic+pcDNA3.1 group, $^{\&}P<0.05$; n=3.

and promote osteoblast apoptosis ($P<0.05$). It indicated that the inhibitory effect of sh-HAGLR on osteoblast growth could be partially saved by BMP2 ($P<0.05$).

HAGLR promoted bone healing in TF mice

Then, HE staining was used for the histological observation. The results showed that the shapes of the calluses in the tibias in the Sham group (n=5) were regular and compact on the 21st day after the transplantation. Under a high power microscope, we observed that the bone cells were mature, small in size, and that there was no significant woven bone (**Figure 7Aa**). However, in the TF group (n=5), there were many braided bones at the fracture site, and the arrangement was irregular. At high magnification, a large number of bone cells were deposited in the bone matrix (**Figure 7Ab**). Compared with the TF group, the tissue morphology of the TF+pcDNA3.1-HAGLR group

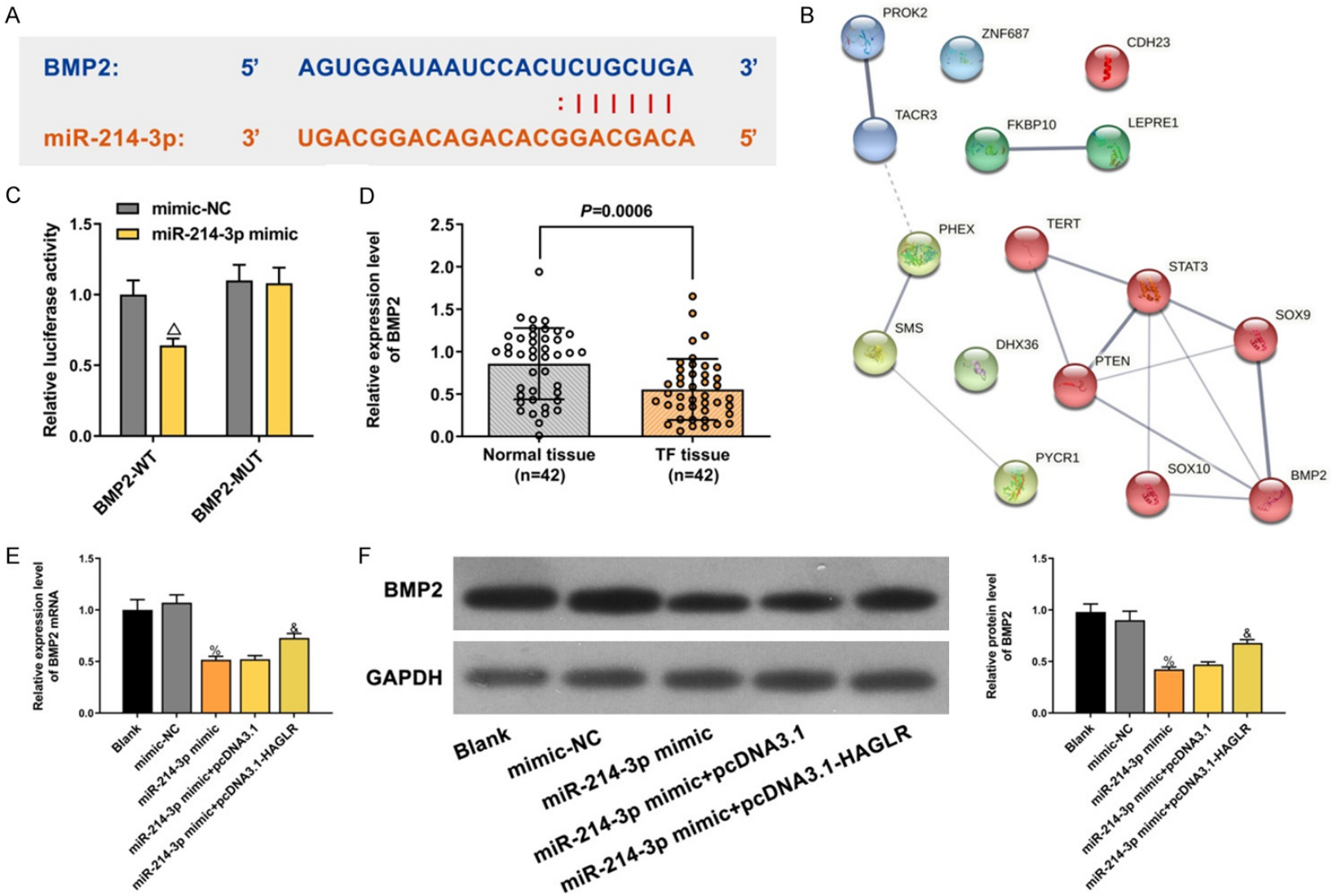

Figure 5. lncRNA HAGLR regulated the expression of its direct target BMP2 in TF by absorbing miR-214-3p. A: From the StarBase database (http://starbase.sysu.edu.cn/index.php), we found that BMP2 is a direct target of miR-214-3p; B: The interaction between BMP2 and the first 15 risk genes associated with increased fracture probability; C: A dual-luciferase report experiment verifies the relationship between BMP2 and miR-214-3p; D: The BMP2 expressions in the TF tissues (n=42) and the adjacent healthy tissues (n=42) were tested using qRT-PCR; E: The BMP2 mRNA level in the MC3T3-E1 cells was measured using qRT-PCR; F: The BMP2 protein level in the MC3T3-E1 cells was measured using WB; Compared with the mimic-NC and the BMP2-WT co-transfection group, $^{\Delta}P<0.05$; compared with the mimic-NC group, $^{\%}P<0.05$; compared with the miR-214-3p mimic+pcDNA3.1 group, $^{\&}P<0.05$; n=3.

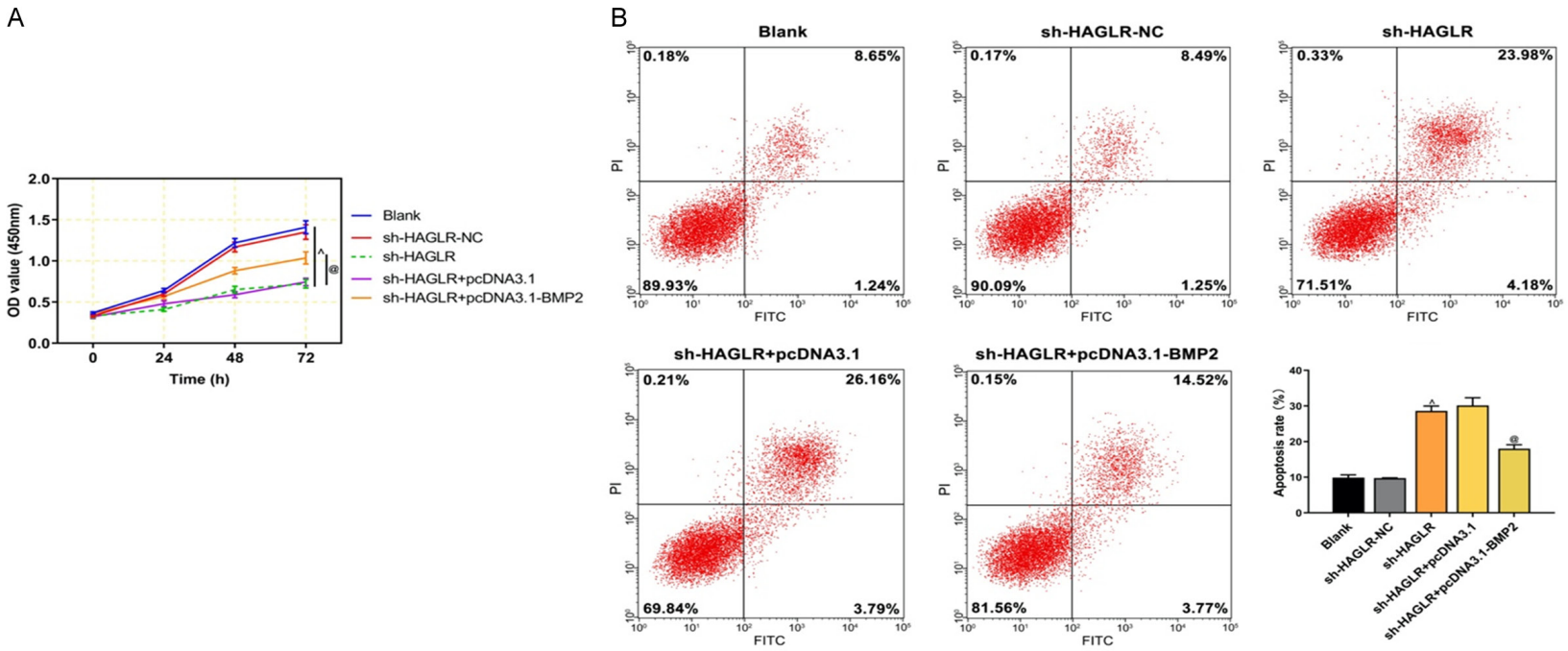

Figure 6. The role of BMP2 in osteoblast growth. A: MTT assays were used to measure the cell proliferation. B: The apoptosis was measured using flow cytometry. Compared with the sh-HAGLR-NC group, ^P<0.05; Compared with the sh-HAGLR-NC+pcDNA3.1 group, @P<0.05; n=3.

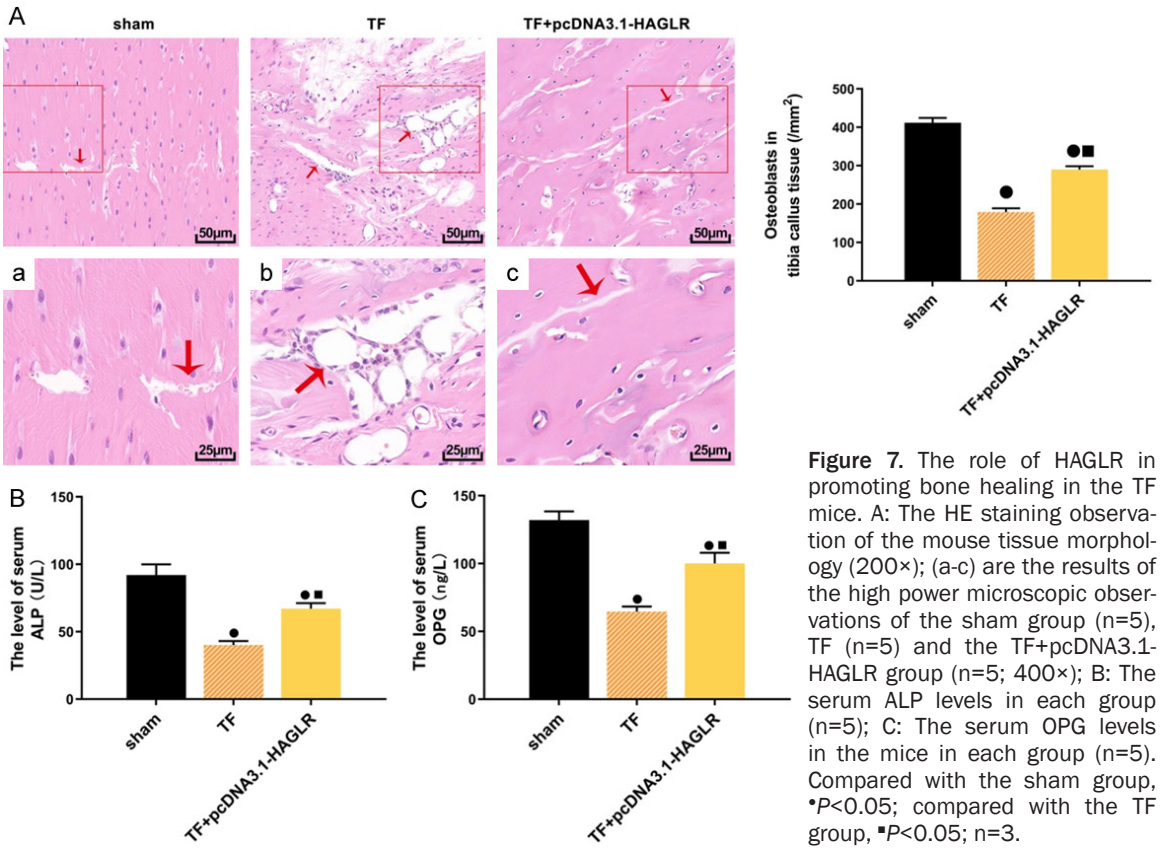

Figure 7. The role of HAGLR in promoting bone healing in the TF mice. A: The HE staining observation of the mouse tissue morphology (200×); (a-c) are the results of the high power microscopic observations of the sham group (n=5), TF (n=5) and the TF+pcDNA3.1-HAGLR group (n=5; 400×); B: The serum ALP levels in each group (n=5); C: The serum OPG levels in the mice in each group (n=5). Compared with the sham group, •P<0.05; compared with the TF group, ▪P<0.05; n=3.

(n=5) was improved. At high magnification, bone trabecula and chondrocytes were formed (**Figure 7Ac**). In addition, compared with the number of osteoblasts per square millimeter of the tibial callus in each group, we found that the number of osteoblasts in the sham group was lower than the number in the TF group (n=5), and it was improved after the addition of HAGLR (**Figure 7A**). The ALP and OPG expression levels in the mouse models were measured using ELISA to evaluate the regulatory effect of HAGLR on the bone healing in the TF mice. Compared with the sham group (n=5), the serum ALP and OPG levels in the TF group (n=5) were down-regulated (**Figure 7B**, **7C**, P<0.05). Compared with the TF group, the levels in the mice in the pcDNA3.1-HAGLR group (n=5) increased (P<0.05).

Discussion

In this study, the value of LncRNA HAGLR in promoting TF healing was verified using *in vivo* and *in vitro* experiments. This effect may be achieved through the miR-214-5p/BMP2 axis, which provides a new target for diagnosis and treatment. The osteoblast MC3T3-E1 cells were chosen as our research focus to investigate the effect of lncRNA HAGLR on the proliferation and apoptosis of osteoblasts. In the process of fracture healing, bone cells can differentiate into osteoblasts to form a repair matrix [16]. Hence, osteoblasts play a vital role in the fracture repair process [17]. We found that HAGLR can improve the proliferative activity of the osteoblasts and inhibit their apoptosis. Moreover, the mouse TF model was established with reference to previous experiments, and the effect of HAGLR on the protein ALP and OPG levels was observed; that is, the improvement in fracture healing [18]. ALP and OPG synthesized by osteoblasts were secreted into a bone-specific extracellular matrix during the biological process of ossification, forming a mature bone matrix [19]. Experimental and clinical studies have proved that the contents of ALP and OG in the osteoblasts are commensurate with the number of calluses, and the total ALP will peak around the 21st day. Cartilage callus is formed at the fracture site and transformed into new bone through the ossification process. The results of this study confirmed

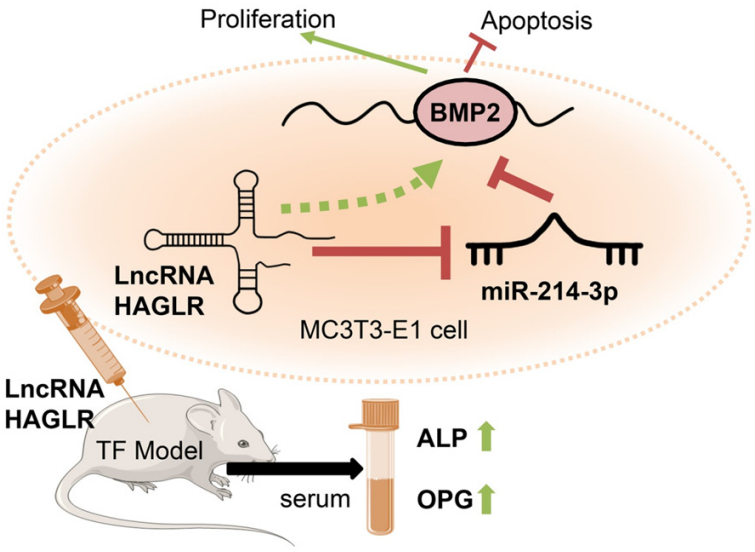

Figure 8. The mechanism by which LncRNA HAGLR absorbs miR-214-3p to promote the BMP2 expression to improve tibial fractures.

that injecting HAGLR can significantly promote the healing and remodeling of TF and increase the serum levels of the bone markers ALP and OG [20].

HAGLR, an lncRNA, can act as a natural miRNA sponge and inhibit gene expression at the post-transcriptional level through the endogenous competition of miRNA binding sites [21]. Next, to explore the specific molecular mechanism of HAGLR in TF, FISH showed that it was mainly expressed in the cytoplasm, suggesting that it can play a role as ceRNA. The miR-214-3p with a potential binding site was found in the StarBase database. Research has confirmed that the miR-214 expression is down-regulated during the osteogenic differentiation of human bone marrow mesenchymal stem cells, suggesting that it may inhibit bone anabolism [22]. Furthermore, transfecting the exosomes of miR-214-3p can effectively reduce the angiogenesis potential. Angiogenesis is one of the key events in the process of bone healing. Over-expressing miR-214-3p in endothelial cells can reduce tubular cell formation and migration, thus inhibiting bone healing [23]. In a word, miR-214-3p can be used as a therapeutic target to improve TF. Next, we verified the targeted binding relationship between miR-214-3p and HAGLR in a dual-luciferase report experiment. In view of a series of functional tests and rescue experiments, miR-214-3p can inhibit the proliferation of osteoblasts and induce their apoptosis, but over-expressing HAGLR can partially rescue the inhibition of miR-214-3p on the osteoblasts.

BMP2 plays a crucial role in promoting the differentiation of osteoporotic osteoblasts [24]. It can boost osteogenic differentiation of bone marrow mesenchymal stem cells, thus slowing down the progress of osteoporosis [25]. It can also increase the OPG secretions of osteoblasts, thus promoting fracture healing [26].

In this experiment, we established and verified the lncRNA HAGLR/miR-214-3p/BMP2 axis. BMP2 is down-regulated in TF tissues, which could save sh-HAGLR from weakening osteoblast proliferation and inducing apoptosis. Also, it has a positive significance for osteoblast growth, thus relieving TF. This study research has certain limitations for further exploring the mechanism. For instance, first of all, the ALP and OPG levels were only detected in the serum as a method for evaluating TF healing. Next, the number of cases included was small. Finally, the downstream signal path was not further explored.

To sum up, lncRNA HAGLR up-regulates BMP2 expression by sponging miR-214-3p, thus improving the progression of TF. On the basis of the experimental results, we believe that lncRNA HAGLR may be a promising target for fracture treatment, which is crucial for bone tissue repair and promoting the healing of TF. This also helps to clarify the specific mechanism of HAGLR in promoting TF healing by regulating BMP2 and absorbing miR-214-3p. In this study, the bioinformatic analytical methods are more diverse and precise with the combined application of a variety of technologies. The schematic diagram of this study is shown in **Figure 8**.

Disclosure of conflict of interest

None.

Address correspondence to: Yishan Yang, Department of Orthopedics, Zhangzhou Affiliated Hospital

of Fujian Medical University, No. 59 Shengli West Road, Xiangcheng District, Zhangzhou 363000, Fujian Province, China. Tel: +86-13695970699; E-mail: a13695970699@126.com

References

[1] Shimberg JL, Aoyama JT, Leska TM, Ganley TJ, Fabricant PD, Patel NM, Cruz AI Jr, Ellis HB Jr, Schmale GA, Green DW, Jagodzinski JE, Kushare I, Lee RJ, McKay S, Rhodes J, Sachleben B, Sargent C, Yen YM and Mistovich RJ. Tibial spine fractures: how much are we missing without pretreatment advanced imaging? A multicenter study. Am J Sports Med 2020; 48: 3208-3213.

[2] Li WW, Yang Y, Shi XY, Guo TZ, Guang Q, Kingery WS, Herzenberg LA and Clark JD. Germinal center formation, immunoglobulin production and hindlimb nociceptive sensitization after tibia fracture. Brain Behav Immun 2020; 88: 725-734.

[3] Zhang T, Han W, Zhao K, Yang W, Lu X, Jia Y, Qin A and Qian Y. Psoralen accelerates bone fracture healing by activating both osteoclasts and osteoblasts. FASEB J 2019; 33: 5399-5410.

[4] Chen P, Gu WL, Gong MZ, Wang J and Li DQ. GIT1 gene deletion delays chondrocyte differentiation and healing of tibial plateau fracture through suppressing proliferation and apoptosis of chondrocyte. BMC Musculoskelet Disord 2017; 18: 320.

[5] McNamara IR, Smith TO, Shepherd KL, Clark AB, Nielsen DM, Donell S and Hing CB. Surgical fixation methods for tibial plateau fractures. Cochrane Database Syst Rev 2015; 9: CD009679.

[6] Silva AM, Moura SR, Teixeira JH, Barbosa MA, Santos SG and Almeida MI. Long noncoding RNAs: a missing link in osteoporosis. Bone Res 2019; 7: 10.

[7] Pan LX and Ding W. LncRNA HAGLR accelerates femoral neck fracture healing through negatively regulating miRNA-19a-3p. Eur Rev Med Pharmacol Sci 2020; 24: 4080-4087.

[8] Qi Y, Ma N, Yan F, Yu Z, Wu G, Qiao Y, Han D, Xiang Y, Li F, Wang W and Gao X. The expression of intronic miRNAs, miR-483 and miR-483*, and their host gene, Igf2, in murine osteoarthritis cartilage. Int J Biol Macromol 2013; 61: 43-49.

[9] Chen H, Yang J and Tan Z. Upregulation of microRNA-9-5p inhibits apoptosis of chondrocytes through downregulating Tnc in mice with osteoarthritis following tibial plateau fracture. J Cell Physiol 2019; 234: 23326-23336.

[10] Teng JW, Ji PF and Zhao ZG. MiR-214-3p inhibits β-catenin signaling pathway leading to delayed fracture healing. Eur Rev Med Pharmacol Sci 2018; 22: 17-24.

[11] Dudakovic A, Samsonraj RM, Paradise CR, Galeano-Garces C, Mol MO, Galeano-Garces D, Zan P, Galvan ML, Hevesi M, Pichurin O, Thaler R, Begun DL, Kloen P, Karperien M, Larson AN, Westendorf JJ, Cool SM and van Wijnen AJ. Inhibition of the epigenetic suppressor EZH2 primes osteogenic differentiation mediated by BMP2. J Biol Chem 2020; 295: 7877-7893.

[12] Zeng HC, Bae Y, Dawson BC, Chen Y, Bertin T, Munivez E, Campeau PM, Tao J, Chen R and Lee BH. MicroRNA miR-23a cluster promotes osteocyte differentiation by regulating TGF-β signalling in osteoblasts. Nat Commun 2017; 8: 15000.

[13] Guo PY, Wu LF, Xiao ZY, Huang TL and Li X. Knockdown of MiR-140-5 promotes osteogenesis of adipose-derived mesenchymal stem cells by targeting TLR4 and BMP2 and promoting fracture healing in the atrophic nonunion rat model. Eur Rev Med Pharmacol Sci 2019; 23: 2112-2124.

[14] Song X, Huang X, Yakufu M, Yan B and Feng C. Minimally invasive plate osteosynthesis or conventional intramedullary nailing for distal tibial fractures: a cohort study protocol. Medicine (Baltimore) 2020; 99: e21779.

[15] Zhu L, Lin ZW, Wang G, Zhang H, Liu B and Xu QJ. MicroRNA-495 downregulates AQP1 and facilitates proliferation and differentiation of osteoblasts in mice with tibial fracture through activation of p38 MAPK signaling pathway. Sci Rep 2019; 9: 16171.

[16] Wang X, Wang C, Gou W, Xu X, Wang Y, Wang A, Xu W, Guo Q, Liu S, Lu Q, Meng H, Yuan M, Peng J and Lu S. The optimal time to inject bone mesenchymal stem cells for fracture healing in a murine model. Stem Cell Res Ther 2018; 9: 272.

[17] Zhu C, Sha M, Jiang H, Lin J, Lin W, Li W, Chen X, Huang G and Ding Z. Co-culture of the bone and bone marrow: a novel way to obtain mesenchymal stem cells with enhanced osteogenic ability for fracture healing in SD rats. J Orthop Surg Res 2019; 14: 293.

[18] Shi E, Chen G, Qin B, Yang Y, Fang J, Li L, Wang Y, Zhu M, Yang J and Gu L. A novel rat model of tibial fracture for trauma researches: a combination of different types of fractures and soft tissue injuries. J Orthop Surg Res 2019; 14: 333.

[19] Zheng H, Qi S and Chen C. Salidroside improves bone histomorphology and prevents bone loss in ovariectomized diabetic rats by upregulating the OPG/RANKL ratio. Molecules 2018; 23: 2398.

[20] Gu H, Li Z, Lv XF, Zhao AB, Zhu MY and Zhang Y. LncRNA KCNQ1OT1 delayed fracture healing

through the Wnt/β-catenin pathway. Eur Rev Med Pharmacol Sci 2019; 23: 4575-4583.
[21] Tay Y, Rinn J and Pandolfi PP. The multilayered complexity of ceRNA crosstalk and competition. Nature 2014; 505: 344-352.
[22] Li L, Fang J, Liu Y and Xiao L. LncRNA LOC100506178 promotes osteogenic differentiation via regulating miR-214-5p-BMP2 axis in human bone marrow mesenchymal stem cells. PeerJ 2020; 8: e8909.
[23] Wang X, Li X, Li J, Zhai L, Liu D, Abdurahman A, Zhang Y, Yokota H and Zhang P. Mechanical loading stimulates bone angiogenesis through enhancing type H vessel formation and downregulating exosomal miR-214-3p from bone marrow-derived mesenchymal stem cells. FASEB J 2021; 35: e21150.
[24] Xiong Y, Chen L, Yan C, Endo Y, Mi B and Liu G. The lncRNA Rhno1/miR-6979-5p/BMP2 axis modulates osteoblast differentiation. Int J Biol Sci 2020; 16: 1604-1615.
[25] Zhang N, Hu X, He S, Ding W, Wang F, Zhao Y and Huang Z. LncRNA MSC-AS1 promotes osteogenic differentiation and alleviates osteoporosis through sponging microRNA-140-5p to upregulate BMP2. Biochem Biophys Res Commun 2019; 519: 790-796.
[26] Ma X, Yang J, Liu T, Li J, Lan Y, Wang Y, Wang A, Tian Y and Li Y. Gukang capsule promotes fracture healing by activating BMP/SMAD and Wnt/β-catenin signaling pathways. Evid Based Complement Alternat Med 2020; 2020: 7184502.